Relativistic Effects in Gold Chemistry. 4. Gold(III) and Gold(V) Compounds

Peter Schwerdtfeger,* Peter D. W. Boyd, Stephane Brienne, and Anthony K. Burrell†

Department of Chemistry, University of Auckland, Private Bag 92091, Auckland, New Zealand, and Research School of Chemistry, The Australian National University, G.P.O. Box 4, Canberra, ACT 2601, Australia

Received September 9, 1991

Hartree–Fock (HF) calculations of the electronic structure and bonding in gold(III) and gold(V) compounds (AuH_3, AuF_3, $AuCl_3$, AuH_4^-, AuF_4^-, $AuCl_4^-$, $AuBr_4^-$, AuI_4^-, AuF_6^-, Au_2H_6, Au_2F_6, Au_2Cl_6) have been carried out. Nonrelativistic and relativistic pseudopotentials were applied using a [Xe4f^{14}]-core definition for the gold atom, however, including the 5s and 5p electrons in the valence space. All bond distances and angles were optimized. Møller–Plesset (MP2-4) calculations on the stability of gold(III) halide complexes were carried out to study the effects of electron correlation at the nonrelativistic and relativistic level of the theory. The relativistic effects in the Au–L bond are analyzed. Relativistic changes in Au(III)–ligand bond distances are calculated to be small compared to those in Au(I) compounds. However, relativistic changes in Au(III)–ligand stretching force constants are very large and of comparable magnitude to that in Au(I) compounds. The preference of the oxidation state III in gold is found to be influenced considerably by relativistic effects and is dependent on the electronegativity of the ligand. The conclusions drawn from previously published HF results (*J. Am. Chem. Soc.* **1989**, *111*, 7261) on the stability of AuL_4^- (L = F, Cl, Br, I) are confirmed by MP2-4 calculations; i.e., the decomposition $AuL_4^- \rightarrow AuL_2^- + L_2$ occurs less easily relativistically than nonrelativistically. Relativistic effects also contribute to the facile decomposition of AuF into Au and AuF_3. All calculated AuL_3 compounds (L = H, F, Cl) show T-shaped structures as a result of a first-order Jahn–Teller symmetry breaking of the D_{3h} trigonal planar structure into the C_{2v} arrangement. A rationalization for the polymeric helix structure of AuF_3 is provided. The stability and structure of gold(III) hydride is examined in detail. Multiple scattering Xα calculations were carried out on AuF_4^-, $AuCl_4^-$, $AuBr_4^-$, and AuI_4^- to determine relativistic effects in the nuclear quadrupole coupling constant for ^{197}Au. Au_2Cl_6 was prepared, and a single-crystal X-ray analysis was carried out to compare with data obtained by the MP2 method (monoclinic, space group $P2_1/c$ with a = 6.5906 (9) Å, b = 11.007 (2) Å, c = 6.442 (3) Å, Z = 4, 873 reflections, and R = 0.0561).

1. Introduction

The stability of the oxidation state III in gold is unique in the group 11 series. Grimm and Sommerfeld pointed out as early as 1926 that the copper and gold atomic core seem to be less stable than that of silver.[1] It is well-known, for example, that Au(I) and Cu(I) compounds disproportionate in aqueous solution according to the equations

$$2Cu^+ \rightarrow Cu + Cu^{2+}$$

$$3Au^+ \rightarrow 2Au + Au^{3+}$$

unless the oxidation state +1 is stabilized by complexation.[2] This fact is often explained by the series of ionization energies: $M \rightarrow M^+ \rightarrow M^{2+} \rightarrow M^{3+}$.[2] Figure 1 shows that the first ionization energy is smallest in silver, the second ionization energy is smallest in copper, and the third ionization energy is smallest in gold. Simply, this reflects the preferred oxidation states in the inorganic group 11 compounds. One may then argue that, as a result of this behavior, AuF and AuF_2^- are not known but AuF_3 and AuF_4^- have been isolated.[2,6] The oxidation state +2 in gold is very rare, and only recently a few, mainly dinuclear, gold(II) compounds have been isolated.[7] These differences in stability of oxidation states within the group 11 elements play a crucial role, for example, in superconductivity. $La_{2-x}Sr_xCuO_4$ is well-known to be a high-temperature superconductor.[8] Although, the mechanism of this phenomenon is still not clear, copper atoms in the oxidation state +2 may play a key role.[9] High-temperature superconductors of silver and gold are unknown so far,[8] which may be the consequence of the instability of the oxidation state +2 for these elements.

We point out that the differences in oxidation states interpreted by the sequence in ionization potentials is influenced by relativistic effects as shown in Figure 1. The trend in the ionization potentials from gold to copper is better described at the Dirac–Fock (DF) level, but relativistic effects do not change the overall behavior. For example, the ionization $M^{2+} \rightarrow M^{3+}$ is lowest for gold at both the nonrelativistic and the relativistic level of the theory (Figure 1c). Because oxidation numbers in chemical compounds do not correspond to measurable quantities (even if they are useful), the stability of compounds in these oxidation states should be explained better by use of quantum chemical concepts such as the relativistic Hartree–Fock (HF) method. The sequence in ionization energies cannot explain why AuI_2^- is stable at room temperature but AuI_4^-

*To whom correspondence should be addressed at the University of Auckland.

† Present address: Department of Chemistry, University of Texas at Austin, Austin, TX.

(1) Grimm, H. G.; Sommerfeld, A. *Z. Phys.* **1926**, *36*, 36.
(2) (a) Puddephatt, R. J. *The Chemistry of Gold*; Elsevier: Amsterdam, 1978. (b) Puddephatt, R. J. In *Comprehensive Organometallic Chemistry*; Wilkinson, G., Stone, F. G. A., Abel, E. W., Eds.; Pergamon: Oxford, 1982; Vol. 15, p 765. (c) Puddephatt, R. J. In *Comprehensive Coordination Chemistry*; Pergamon: Oxford, England, 1987; Vol. 5, p 861. (d) Uson, R.; Laguna, A. *Coord. Chem. Rev.* **1986**, *70*, 1.
(3) Moore, C. E. *Atomic Energy Levels*; Natl. Bur. Stand. (U.S.) Circ. No. 467; U.S. GPO: Washington, DC, 1958.
(4) (a) Froese-Fischer, C. *Comp. Phys. Commun.* **1978**, *14*, 145. (b) Froese-Fischer, C. *The Hartree-Fock Method for Atoms*; Wiley: New York, 1977.
(5) (a) Grant, I. P.; McKenzie, B. J.; Norrington, P. H.; Mayers, D. F.; Pyper, N. C. *Comp. Phys. Commun.* **1980**, *21*, 207. (b) McKenzie, B. J.; Grant, I. P.; Norrington, P. H. *Comp. Phys. Commun.* **1980**, *21*, 233. (c) McKenzie, B. J.; Grant, I. P.; Norrington, P. H. *Comp. Phys. Commun.* **1981**, *23*, 222.
(6) Müller, B. G. *Angew. Chem., Int. Ed. Engl.* **1987**, *26*, 1081; *Angew. Chem.* **1987**, *99*, 1120.
(7) Silver, J. In *Annu. Rep. A* **1986**, *83*, 333.
(8) Wolf, S. A.; Kresin, V. Z. *Novel Superconductivity*; Plenum: New York, 1987.
(9) Chen, G.; Goddard, W. A., III. *Science* **1988**, *26*, 1081.

0020-1669/92/1331-3411$03.00/0

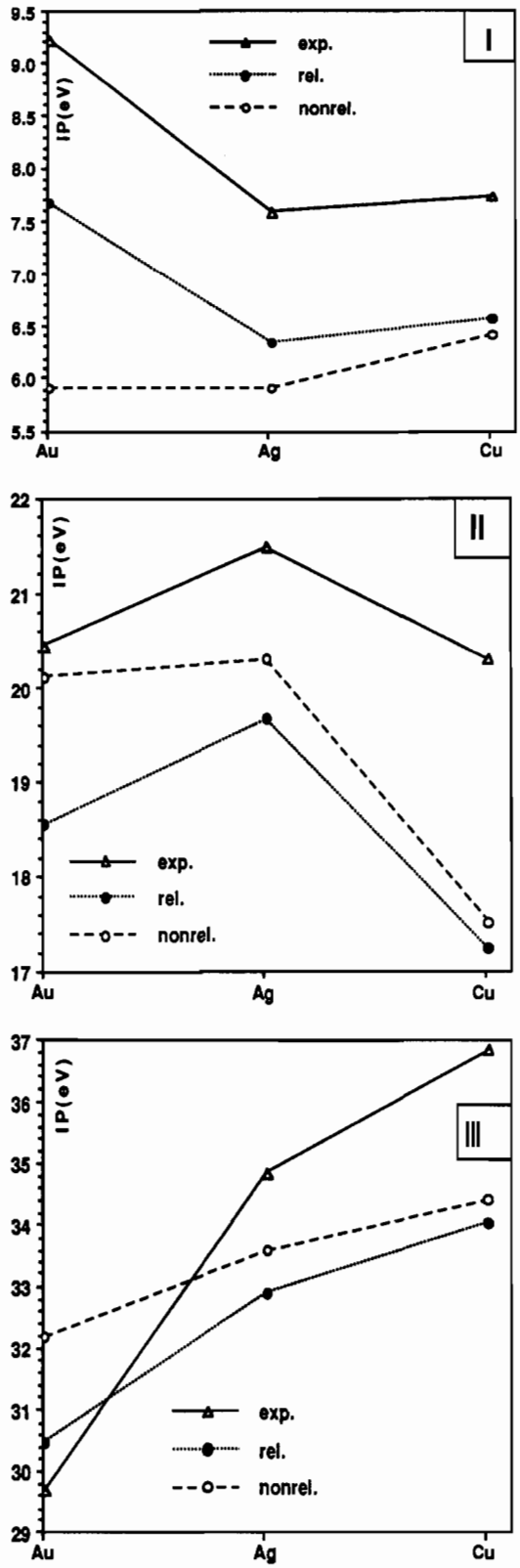

Figure 1. HF ionization potentials for copper, silver, and gold (in eV): I, $M(^2S_{1/2}) \rightarrow M^+(^1S_0)$; II, $M^+(^1S_0) \rightarrow M^{2+}(^2D_{5/2})$; III, $M^{2+}(^2D_{5/2}) \rightarrow M^{3+}(^3F_4)$. Experimental data are from ref 3. The HF values have been calculated by using the program MCHF;[4] the DF values have been calculated by using the program MCDF/BENA including major QED effects.[5]

has never been isolated. The stability of higher oxidation states seems to be dependent on the nature of the ligand.

Au(III) is regarded as a harder Lewis acid than Au(I),[2] and the chemistry of Au(III) is more extensive than that of Au(I). The most common coordination numbers of gold compounds in the higher oxidation states are 4 and 6, either in square planar or in octahedral geometry. The neutral monomers AuL_3 (L any ligand) have never been detected in the gas phase, indicating that the coordination number 3 is not favored (with some exceptions like $[Au(PPh_3)_3]^+$). Hence, such compounds have a tendency to add a fourth ligand to form the stable AuL_4^- complex or to bridge with other AuL_3 compounds. For example, $AuCl_3$ has a dimeric chlorine-bridged structure in the solid as well as in the gas phase and compounds like $AuF_3 \cdot SeF_4$ have to be heated to 350 °C to release AuF_3, which in the solid state is a fluorine-bridged helical chain polymer.[2] The reason for the polymerization of AuL_3 compounds is not understood, and we analyze this in detail for the two compounds AuF_3 and $AuCl_3$. We have redetermined the single-crystal X-ray structure for Au_2Cl_6 because the geometry of this compound was determined more than 30 years ago[10] using film data.

Nuclear quadrupole resonance and Mössbauer spectroscopy have been very useful in the analysis of bonding in several gold compounds.[2,11] Electric field gradients (EFG) for Au(I) compounds have been studied in detail by the multiple scattering $X\alpha$ ($MSX\alpha$) method,[12] but Au(III) compounds have not been treated theoretically so far. An unusually high NQCC has been found for ^{197}Au in AuCl,[13] and other gold compounds show electric field gradients at the metal center which are unexpectedly larger than those in corresponding copper species.[11] This has been interpreted in terms of Au(6p) participation in the gold–ligand bond.[11-13] However, it has been shown recently that relativistic effects in EFGs play an important role even in copper compounds[14] and very large relativistic effects have been calculated in the ^{35}Cl NQCC of $AuCl_2^-$.[15] One may therefore expect similar large relativistic effects in $AuCl_4^-$, which will be analyzed at the Hartree–Fock (HF) level.

In our previous three papers of this series[15-18] we presented HF and configuration interaction (CI) calculations using multielectron-adjusted nonrelativistic and relativistic pseudopotentials for gold. We showed that relativistic effects strongly influence physical and chemical properties of gold and its compounds.[15-19] Only very few theoretical studies on Au(III) compounds are available,[20-23] because ab-initio calculations on such compounds with adequate basis sets require a lot of computer time. The halide complexes of Au(III) have been calculated by a semiempirical charge and configuration (SCCC) method.[20] Hoffmann and co-workers[21] studied organogold(III) compounds by means of the extended Hückel method. Recently, Miyoshi and Sakai[22] carried out HF and CI calculations on hexafluoroaurates, AuF_6^{n-}

(10) Clark, E. S.; Templeton, D. H.; MacGillavry, C. H. *Acta Crystallogr.* **1958**, *11*, 284.
(11) Bowmaker, G. A. In *Spectroscopy of Inorganic-based Materials*; Clark, R. J. H., Hester, R. E., Eds.; Wiley: New York, 1987; p 1.
(12) Bowmaker, G. A.; Boyd, P. D. W.; Sorrensen, R. J. *J. Chem. Soc., Faraday Trans. 2* **1985**, *81*, 1627.
(13) (a) Machmer, P. *Z. Naturforsch.* **1966**, *21*, 1966. (b) Machmer, P. *Inorg. Nucl. Chem. Lett.* **1967**, *3*, 215. (c) Machmer, P. *Inorg. Nucl. Chem.* **1968**, *30*, 2627.
(14) Schwerdtfeger, P.; Aldridge, L. P.; Boyd, P. D. W.; Bowmaker, G. A. *Struct. Chem.* **1990**, *1*, 405.
(15) Schwerdtfeger, P.; Boyd, P. D. W.; Burrell, A. K.; Robinson, W. T.; Taylor, M. J. *Inorg. Chem.* **1990**, *29*, 3593.
(16) Schwerdtfeger, P.; Dolg, M.; Schwarz, W. H. E.; Bowmaker, G. A.; Boyd, P. D. W. *J. Chem. Phys.* **1989**, *91*, 1762.
(17) (a) Schwerdtfeger, P.; Dolg, M. *Phys. Rev. A* **1991**, *43*, 1644. (b) Schwerdtfeger, P.; Boyd, P. D. W. *Inorg. Chem.* **1992**, *31*, 327.
(18) Schwerdtfeger, P. *J. Am. Chem. Soc.* **1989**, *111*, 7261.
(19) (a) Pyykkö, P. *Chem. Rev.* **1988**, *88*, 563. (b) Pyykkö, P. *Adv. Quantum Chem.* **1978**, *11*, 353. (c) Schwarz, W. H. E. In *Theoretical Models of Chemical Bonding*; Springer: Heidelberg, Germany, 1989; Vol. 2, p 593.
(20) (a) Zwanziger, H.; Reinhold, J.; Hoyer, E. *Z. Chem.* **1974**, *14*, 489. (b) Basch, H.; Gray, H. B. *Inorg. Chem.* **1967**, *6*, 365.
(21) (a) Komiya, S.; Albright, T. A.; Hoffmann, R.; Kochi, J. K. *J. Am. Chem. Soc.* **1976**, *98*, 7255. (b) Komiya, S.; Albright, T. A.; Hoffmann, R.; Kochi, J. K. *J. Am. Chem. Soc.* **1977**, *99*, 8440. (c) Tatsumi, K.; Hoffmann, R.; Yamamoto, A.; Stille, J. K. *Bull. Chem. Soc. Jpn.* **1981**, *54*, 1857.
(22) Miyoshi, E.; Sakai, Y. *J. Chem. Phys.* **1988**, *89*, 7363.
(23) Boca, R. *Czech. J. Phys.* **1990**, *40*, 629.

Table I. Molecular Properties for the AuL_4^- Complexes (L = H, F, Cl, Br, I) and for AuF_6^- [a]

molecule	method	r_e	D_e	k_e	D_e^1	D_e^2
AuH_4^-	NR HF	1.746	368.6	1.79	274.2	71.1
	R HF	1.652	581.8 (581.8)	2.51	256.9	223.7 (223.7)
AuF_4^-	NR HF	1.980	329.4	3.76	455.0	−81.3
	NR MP2	2.034	982.6	2.05		371.3
	R HF	1.930	523.5 (519.1)	4.23	502.0	116.6 (113.7)
	R MP2	1.974	1144.1 (1139.3)	3.24		488.9 (485.7)
$AuCl_4^-$	NR HF	2.424	327.9	1.86	280.1	−100.1
	NR MP2	2.445	744.6	1.52		225.2
	R HF	2.344	496.4 (485.9)	2.96	342.1	80.3 (73.3)
	R MP2	2.349	896.0 (885.5)	2.17		340.8 (333.8)
$AuBr_4^-$	NR HF	2.580	292.4	1.45		−110.6
	NR MP2	2.579	700.2	1.28		190.7
	R HF	2.492	396.0 (352.9)	2.00		−13.3 (−42.1)
	R MP2	2.486	824.3 (780.2)	2.00		302.9 (273.5)
AuI_4^-	NR HF	2.830	220.3	1.07		−151.5
	NR MP2	2.803	614.1	1.10		148.0
	R HF	2.716	308.2 (217.2)	1.52		−38.9 (−99.6)
	R MP2	2.708	731.2 (640.3)	1.53		236.1 (175.5)
AuF_6^-	NR HF	1.948	−102.2	4.10		−431.6
	NR MP2	2.068	1185.8	1.64		203.2
	R HF	1.903	262.4 (253.6)	4.48		−261.1 (−265.5)
	R MP2	1.984	1409.2 (1401.2)	2.72		265.1 (261.9)

[a] Au–L bond distance r_e in Å, dissociation energy D_e ($AuL_4^- \rightarrow Au + 3L + L^-$) in kJ mol^{-1}, and force constants k_e in mdyn Å^{-1}. D_e^1: $AuL_4^- \rightarrow AuL_3 + L^-$. D_e^2: $AuL_4^- \rightarrow AuL_2^- + 2L$ (for AuF_6^-: $AuF_6^- \rightarrow AuF_4^- + 2F$). The data for AuL_2^- and AuL_3 are collected in Tables II and III, respectively. The spin–orbit-corrected D_e and D_e^2 values are given in parentheses (from atomic $^2P_{1/2}/^2P_{3/2}$ spin–orbit splittings of the halides: corrections for HF values from Dirac–Fock calculations using the program MCDF/BENA[5] and corrections for MP2 values from experiment[3]).

(n = 0–3), employing relativistic pseudopotentials for gold with very small basis sets. No other ab-initio calculations have been reported on Au(III) compounds so far. In this paper we study in detail the relativistic effects in square planar AuL_4^- complexes (L = H, F, Cl, Br, I), in T-shaped AuL_3 compounds (L = H, F, Cl), in the Au(V) complex AuF_6^-, and in the binuclear gold species Au_2H_6, Au_2F_6, and Au_2Cl_6 using HF and Møller–Plesset (MP) procedures.[24] We also calculate the ^{197}Au nuclear quadrupole coupling constants (NQCC) in AuL_4^- complexes (L = F, Cl, Br, I), $AuCl_2^-$, and AuCl using the multiple-scattering Xα (MSXα) method.[25] The methods are described in section 3. The results are presented and discussed in the next section (Tables I–XII and Figures 1–7). A summary is given in section 4.

2. Results and Discussion

A. Molecular Structures. Gold(III) Halide Complexes and AuF_6^-. The calculated bond distances are collected in Table I.

(24) (a) Frisch, M. J.; Binkley, J. S.; Schlegel, H. B.; Raghavachari, K.; Melius, C. F.; Martin, L.; Stewart, J. J. P.; Bobrowicz, F. W.; Rohlfing, C. M.; Kahn, L. R.; DeFrees, D. J.; Seeger, R.; Whiteside, R. A.; Fox, D. J.; Fluder, E. M.; Pople, J. A. Program GAUSSIAN86. Carnegie-Mellon Quantum Chemistry Publishing Unit, Pittsburgh, PA, 1984. Extended for local and nonlocal pseudopotentials by P. Schwerdtfeger using program PSEPOT for the latter: Kolar, M. *Comp. Phys. Commun.* **1981**, *23*, 275. (b) Pople, J. A.; Seeger, R.; Krishnan, R. *Int. J. Quantum Chem. Symp.* **1977**, *11*, 149. (c) Fletcher, R.; Powell, M. J. D. *Comput. J.* **1963**, *6*, 163.

(25) Cook, M.; Case, D. A. Program XASW, VAX-IBM Version 2, personal communication.

(26) Huber, K. P.; Herzberg, G. *Molecular Spectra and Molecular Structure, Constants of Diatomic Compounds*; Van Nostrand: New York, 1979.

(27) Schwerdtfeger, P.; Szentpály, L. v.; Vogel, K.; Silberbach, H.; Stoll, H.; Preuss, H. *J. Chem. Phys.* **1985**, *84*, 1606.

(28) Leavy, K.; Bartlett, N. *J. Chem. Soc., Chem. Commun.* **1972**, 903.

(29) (a) Hendra, P. J. *Spectrochim. Acta* **1966**, *22*, 1483. (b) Hendra, P. J. *J. Chem. Soc. A* **1967**, 1298.

(30) Goggin, P. L.; Mink, J. *J. Chem. Soc., Dalton Trans.* **1974**, 1479.

(31) Tobias, R. S. In *The Raman Effect*; Anderson, A., Ed.; Marcel Dekker: New York, 1973; Vol. 2.

(32) Schwerdtfeger, P.; Bowmaker, G. A.; Boyd, P. D. W.; Earp, C. D.; Hannon, S. F. Program VIB. Department of Chemistry, University of Auckland, Auckland, 1990.

(33) Nakamoto, K. *Infrared and Raman Spectra of Inorganic and Coordination Compounds*; Wiley: New York, 1978.

Table II. MP2 Molecular Properties for the AuL_2^- Complexes (L = F, Cl, Br, I).[a]

molecule	method	r_e	D_e	k_e	D_e^3
AuF_2^-	NR	2.212	611.3	1.32	280.2
	R	2.035	655.2 (653.6)	2.42	382.8
$AuCl_2^-$	NR	2.584	519.4	0.96	231.3
	R	2.332	555.2 (551.7)	1.70	303.1
$AuBr_2^-$	NR	2.659	509.5	0.90	232.3
	R	2.472	521.4 (506.7)	1.64	270.4
AuI_2^-	NR	2.842	466.1	0.79	220.3
	R	2.651	495.1 (464.8)	1.42	268.3
AuF	NR	2.162	331.1	1.91	
	R	2.006	272.4 (270.8)	2.53	
AuCl	NR	2.489	288.1	1.39	
	R	2.287	252.1 (248.6)	2.12	
AuBr	NR	2.597	277.2	1.28	
	R	2.395	251.0 (236.3)	1.99	
AuI	NR	2.773	245.8	1.10	
	R	2.572	226.8 (196.5)	1.77	

[a] Au–L bond distance r_e in Å, dissociation energy D_e ($AuL_2^- \rightarrow Au + L + L^-$) in kJ mol^{-1}, and force constants k_e in mdyn Å^{-1}. D_e^3: $AuL_2^- \rightarrow AuL + L^-$. The spin–orbit-corrected D_e values are given in parentheses (see Table I).

Table III. Molecular Properties for the AuL_3 Complexes (L = H, F, Cl)[a]

L	method	r_e[a]	r_e[c]	α	D_e^1	D_e^2	μ_e
H	NR	1.604	1.753	81.5	94.4	2.1	1.74
	NR MP2	1.604	1.732	82.3	385.0	209.0	1.64
	R	1.492	1.652	86.9	324.9	172.2	0.85
	R MP2	1.485	1.641	86.4	619.6	349.7	0.72
F	NR	1.945	1.939	93.1	−125.6	−288.3	3.97
	R	1.873	1.899	93.3	21.5 (17.1)	−67.1 (-70.0)	3.36
Cl	NR	2.364	2.379	91.8	47.8	−170.1	1.42
	R	2.255	2.289	94.4	154.3 (143.8)	−6.4 (−13.4)	0.88

[a] Au–L bond distance r_e in Å, dissociation energies D_e^1 ($AuL_3 \rightarrow Au + 3L$) and D_e^2 ($AuL_3 \rightarrow AuL + 2L$) in kJ mol^{-1}, and dipole moments μ_e in D. Spin–orbit-corrected values are given in parentheses (see Table I).

Table IV. Relativistic Contributions in Au(III) and Au(V) Compounds per Au–L bond[a]

molecule		$\Delta_R r_e$	$\Delta_R D_e^{SO}$	$\Delta_R k_e$
AuH_3	HF	0.099	−76.7	
	MP2	0.091	−77.9	
AuH_4^-	HF	0.094	−53.3	−0.73
AuF_3	HF	0.046	−47.6	
Au_2F_6	HF	0.040		
AuF_6^-	HF	0.045	−21.1	−0.46
	MP2	0.084	−35.9	−1.08
AuF_4^-	HF	0.050	−47.4	−0.46
	MP2	0.069	−39.2	−1.19
AuF_2^-	MP2	0.177	−21.2	−1.11
AuF	MP2	0.156	+60.3	−0.63
$AuCl_3$	HF	0.090	−32.0	
Au_2Cl_6	HF	0.087		
$AuCl_4^-$	HF	0.080	−39.5	−1.10
	MP2	0.095	−35.2	−0.64
$AuCl_2^-$	MP2	0.252	−8.1	−0.74
AuCl	MP2	0.202	+39.5	−0.72
$AuBr_4^-$	HF	0.088	−15.1	−0.55
	MP2	0.093	−20.0	−0.73
$AuBr_2^-$	MP2	0.187	+1.4	−0.74
AuBr	MP2	0.202	+40.9	−0.71
AuI_4^-	HF	0.114	+0.8	−0.45
	MP2	0.095	−6.6	−0.44
AuI_2^-	MP2	0.191	+0.3	−0.74
AuI	MP2	0.201	+49.3	−0.67

[a] Distances r_e in Å, dissociation energies D_e in kJ mol^{-1} per ligand L (corrected for atomic spin-orbit coupling; see Table I), and force constant k_e in mdyn Å^{-1}. For $\Delta_R r_e$ ligand L_e has been chosen for AuL_3 and Au_2L_6 (L = H, F, Cl).

Structural data for Au(III) compounds have been collected by Melnik and Parish.[34] In all cases Au(III) complexes of the form AuL_4^- show square planar coordination, which is confirmed by

Table V. HF Mulliken Population Analysis for the Au(III) and Au(V) Compounds with Gross Atomic Populations and Total Charges q for the Au Atoms

	NR				R			
molecule	6s	5d	6p	q	6s	5d	6p	q
AuH_3	0.40	9.52	0.24	0.83	1.18	9.30	0.27	0.25
AuH_4^-	0.30	9.48	0.28	0.94	1.04	9.44	0.54	–0.62
Au_2H_6[a]					1.85	9.18	0.01	–0.05
AuF_3	0.31	9.03	0.16	1.56	0.53	8.89	0.32	1.26
AuF_4^-	0.31	8.96	0.20	1.54	0.68	8.80	0.39	1.12
AuF_6^-	0.39	8.55	0.37	1.69	0.38	8.57	0.35	1.70
Au_2F_6	0.32	8.98	0.15	1.56	0.47	8.76	0.30	1.47
$AuCl_3$	0.29	9.45	0.35	0.92	1.16	9.24	0.53	0.06
$AuCl_4^-$	0.25	9.27	0.43	1.05	1.19	9.15	0.66	0.01
Au_2Cl_6	0.38	9.58	0.12	0.91	0.84	9.48	0.54	0.14
$AuBr_4^-$	0.32	9.42	0.53	0.73	1.21	9.18	0.66	–0.05
AuI_4^-	0.42	9.62	0.65	0.31	1.20	9.34	0.71	–0.25

[a] For NR calculations on Au_2H_6 see the text.

our HF geometry optimization. AuF_6^- was calculated to possess an exact octahedral structure with no distortions, as expected. Our calculated MP2 bond distances for the gold(III) halide complexes are in reasonable agreement with results from crystal structure measurements. For example, the Au–F bond distances in $MAuF_4$ vary between 1.85 and 1.95 Å[35] depending on the counterion M^+ (calculated MP2 value 1.97 Å), the Au–F bond distance in $KAuF_6$ is 1.9 Å[36] (HF value 1.92 Å), the Au–Cl bond distance in $AuCl_4^-$ is 2.27–2.30 Å[34] depending on the choice of M^+ (MP2 value 2.35 Å), and the Au–Br bond distance in $AuBr_4^-$ is about 2.43 Å[2] (MP2 value 2.49 Å). Comparable Au–I bond distances for AuI_4^- are not available, but this moiety is contained in $Rb_2AgAu_3I_8$, which has a Au(III)–I bond distance of 2.64 Å[37] (MP2 value 2.71 Å). In all cases, the calculated bond distances exceed the experimental ones by about 0.02–0.07 Å. These differences are due to solid-state effects, the effect of the counterion M^+, and the various approximations used in our calculations.

The nonrelativistic and relativistic MP2 bond distances for the gold(III) halide complexes AuL_4^- are shown in Figure 2 and are compared with those of the Au(I) complexes AuL_2^- and of the diatomic AuL compounds (L = F, Cl, Br, I). We first note that the relativistic bond contraction $\Delta_R r_e$ ($=r_e^{NR} - r_e^R$) decreases from the Au(I) to the Au(III) complexes, $\Delta_R r_e(AuL) \sim \Delta_R r_e(AuL_2^-) > \Delta_R r_e(AuL_4^-)$ ($\sim \Delta_R r_e(AuL_6^-)$ for L = F); i.e., the relativistic bond contractions in Au(III) compounds are about three times smaller than those in the corresponding Au(I) compounds (Table IV). This leads to the conclusion that the anomalous trend in bond lengths pointed out for the diatomic gold compounds[16] should not be observed for group 11 complexes in the oxidation states +3 and +5 (the intra-lanthanide contraction is normally between 0.1 and 0.2 Å depending on the nature of the ligands; see refs 17 and 38). However, only the anions CuF_4^- and AgF_4^- have been synthesized and accurate structural data are not available.[35,36] Hoppe and Hoffmann[36] concluded from powder diffraction studies that $r_e(AgF_4^-) < r_e(AuF_4^-)$, the difference being ~0.1 Å, which agrees with our calculated low relativistic bond contraction. Even AuH_4^- shows a very small relativistic bond contraction of about 0.09 Å at the HF level ($\Delta_R r_e$(AuH) is 0.25 Å at the HF level and 0.29 Å at the CI level[16]). A possible rationalization of the relatively small $\Delta_R r_e$ values calculated for all Au(III) compounds is that the very large Au(5d) and Au(6p) participation in the Au–L bond relative to that in the Au(I) species (cf. Table V and ref 15) dilutes the 6s participation and therefore quenches the bond contraction caused by the relativistic Au(6s) contraction. The relativistic 5d expansion[19] may also contribute (see however ref 39). The very small relativistic bond contraction in Au(III) complexes compared to that in Au(I) compounds[15,16] results in a change in the trend of bond lengths along the series AuL, AuL_2^-, and AuL_4^- (Figure 2). For example, at the nonrelativistic level we find $r_e(AuCl_2^-) > r_e(AuCl_4^-)$, as expected. However, at the relativistic level we have the reverse trend; i.e., $r_e(AuCl_2^-)$ is smaller by about 0.02 Å (MP2) than $r_e(AuCl_4^-)$ (Tables I and II). Indeed, this order has been found in the crystal structure of the mixed complex $Cs_2[AuCl_2][AuCl_4]$.[40]

$(AuF_3)_n$ and $(AuCl_3)_n$. The following definition of the ligands of AuL_3 and Au_2L_6 (L = H, F, Cl) is used in the tables and text:

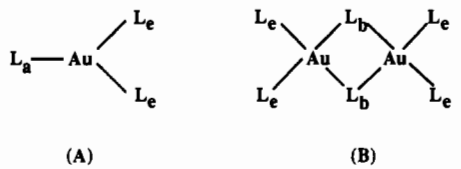

(A) (B)

The structural data for the dinuclear gold compounds Au_2H_6, Au_2F_6, and Au_2Cl_6 are given in Table VI. Crystal data details of the Au_2Cl_6 structure determination, final observed and calculated structure factors, the final refined atomic coordinates and thermal parameters of the gold and chlorine atoms, and bond lengths and angles in the dimeric unit are given in Table VII and in the supplementary material. Figure 3 shows the dimeric unit present in the crystal structure. The structure and unit cell of Au_2Cl_6 shown in these tables do not differ much from those reported by Clark et al.,[10] although the accuracy of the structure refined from diffractometer data is improved; the final values are $R = 0.0561$ and $R_w = 0.0602$. The HF geometry is not in very good agreement with our experimentally measured crystal structure with deviations of more than 0.15 Å for the Au–Cl_b distance. This leads to an error in the Au–Au distance of more than 0.25 Å. We therefore performed an MP2 optimization for this compound, which slightly improves the agreement between calculation and experiment. In these calculations polarization functions for the chlorine atoms were left out since even the HF calculations have been very time consuming in CPU.[41] Cl(d) functions are expected to shorten the Au–Cl distance significantly, and their inclusion would improve the agreement even further. This can be seen by comparison of the $AuCl_3$ calculations with

(34) Melnik, M.; Parish, R. V. *Coord. Chem. Rev.* **1986**, *70*, 157.
(35) (a) Edwards, A. J.; Jones, G. R. *J. Chem. Soc. A* **1969**, 1936. (b) Engelmann, U.; Müller, B. G. *Z. Anorg. Allg. Chem.* **1990**, *589*, 51.
(36) (a) Hoppe, R.; Hoffmann, R. *Z. Anorg. Allg. Chem.* **1970**, *379*, 193. (b) Hoppe, R.; Klemm, W. *Z. Anorg. Allg. Chem.* **1952**, *268*, 364. (c) Hoppe, R. *Z. Anorg. Allg. Chem.* **1957**, *292*, 28. (d) Fleischer, T.; Hoppe, R. *Z. Anorg. Allg. Chem.* **1982**, *492*, 76. (e) Engelmann, U.; Müller, B. G. *Z. Anorg. Allg. Chem.* **1990**, *589*, 51.
(37) Werner, W.; Strähle, J. *Z. Naturforsch.* **1979**, *B34*, 952.
(38) Pyykkö, P. Personal communication, 1990.
(39) (a) Snijders, J. G.; Pyykkö, P. *Chem. Phys. Lett.* **1980**, *75*, 5. (b) Schwarz, W. H. E. *Phys. Scr.* **1987**, *36*, 403.
(40) Eijnhoven, J. C. M. T.; Verschoor, G. C. *Mater. Res. Bull.* **1974**, *9*, 1667.
(41) For Au_2Cl_6 we took a (8s,5p,4d)/[7s,2p,3d] for Au and a 6-621G basis set for Cl (a total of 338 basis functions contracted to 134). This produced about 11 million 2-electron integrals. A total geometry optimization required about 100-h CPU on an IBM3081 computer.

Table VI. Molecular Properties for the Au_2L_6 Compounds (L = H, F, Cl)[a]

molecule	method	$r_e^{Au-L_a}$	$r_e^{Au-L_b}$	r_e^{Au-Au}	$\alpha_e^{L_aAuL_a}$	$\alpha_e^{L_bAuL_b}$	D_e	ΔU_0
Au_2H_6[d]	NR	2.09	2.09	2.91	21	92	<-700	
	R	1.559	1.857	2.772	71.4	83.4	206.8	-10.3
Au_2F_6	NR	1.941	2.115	3.377	89.1	74.0	283.7	147.5
	R	1.894	2.071	3.289	90.0	74.8	337.4	2.7
AuF_3	NR	1.957	1.970			172.4		
	R	1.901	1.918			174.0		
Au_2Cl_6	NR	2.414	2.592	3.868	82.9	83.5	158.3	165.4
	R	2.327	2.490	3.682	88.4	84.6	189.2	55.4
	RMP2	2.367	2.483	3.617	88.7	86.5		
	exptl[b]	2.23	2.33	3.41	90	86		
	exptl[c]	2.243	2.334	3.422	89.9	85.9		
$AuCl_3$	NR	2.428	2.429			179.1		
	R	2.322	2.343			174.1		

[a] Reduced basis sets are used for F and Cl; e.g., compare with Table III for the AuL_3 compounds. Au–L bond distance r_e in Å, bond angles α_e in deg, and dissociation energy D_e ($Au_2L_6 \rightarrow 2AuL_3$) in kJ mol^{-1}. See text for the ligand definitions. ΔU_0 given for the reaction $6AuL \rightarrow Au_2L_6 + 2Au_2$ (in kJ (mol of AuL)$^{-1}$). [b] Reference 10. [c] Our work. [d] NR geometry not fully optimized for Au_2H_6; see text.

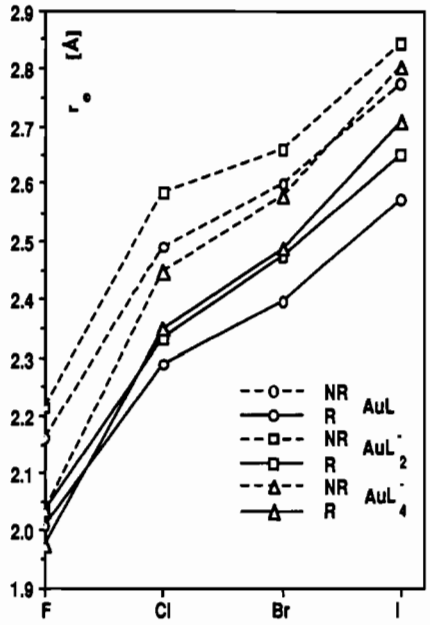

Figure 2. Nonrelativistic and relativistic MP2 bond distances (in Å) for the gold halides AuL, AuL_2^-, and AuL_4^- (L = F, Cl, Br, I).

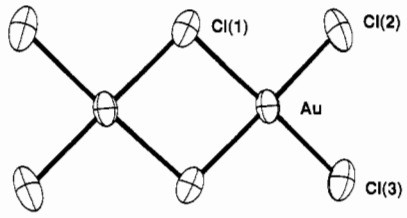

Figure 3. ORTEP representation of the X-ray crystal structure of the molecule Au_2Cl_6.

and without d-polarization functions (cf. Tables III and VI). Inclusion of a Cl(d)-polarization function shortens the Au–Cl bond distances by ~0.06 Å. If we correct our MP2 results for Au_2Cl_6 by this value, we obtain a satisfactory agreement with the experimental Au–Cl bond lengths. The MP2 bond angles are in very good agreement with these obtained from the X-ray measurement. Relativistic changes in bond lengths are small in this compound (~0.1 Å) and comparable to that of $AuCl_4^-$. A large relativistic change (5.6°) is calculated for the L_eAuL_e angle, whereas the L_bAuL_b angle only changes by 1.1° due to relativistic effects.

The structure of AuF_3 in the gas phase is unknown. In the solid state, AuF_3 adopts a helical structure, in which each gold atom is surrounded by six fluoride ligands in a distorted octahedron.[2,42] We may, however, compare to the two bond lengths given in the $(AuF_3)_n$ crystal structure, 1.91 Å for the nonbridged Au–F bond distance and 2.04 Å for the bridged one. Our RHF values of 1.89 and 2.07 Å compare quite well with these numbers. The Au–F_b–Au angle in $(AuF_3)_n$ (116°) differs from our calculated one (97°) due to the different arrangement of the AuF_3 units. This also explains the different measured (3.46 Å) and calculated (3.29 Å) Au–Au bond lengths in $(AuF_3)_n$ and Au_2F_6, respectively. Relativistic changes in the structure are relatively small as expected from the results obtained for AuF_4^- and the one for AuF published previously.[2] The relative small differences in metal–fluorine bond distances between $(AuF_3)_n$ and $(AgF_3)_n$[42b] may therefore be a mixture of both relativistic and lanthanide-contraction effects.

Table VII. Bond lengths (Å) and Angles (deg) for Au_2Cl_6

	Distances		
Au–Cl1	2.334 (10)	Au–Cl2	2.249 (10)
Au–Cl3	2.243 (10)	Au–Au	3.422 (2)
	Angles		
Cl2–Au–Cl1	92.1 (4)	Cl3–Au–Cl1	177.8 (4)
Cl3–Au–Cl2	89.9 (4)	Au–Cl1–Au	93.6 (1)

Inorganic AuL_3 compounds have been postulated to possess a trigonal planar (D_{3h}) arrangement due to gold sp^2 or d^2s hybridization.[2] However, all AuL_3 species calculated show T-shaped structures (C_{2v}) with an L_aAuL_e angle near 90°, 164 kJ/mol below the trigonal planar arrangement (at the RHF level). This could be explained through mixed Au(5d) and Au(6p) admixture in the σ-Au–L bond ("dsp-hybridization").[43] Indeed, the population analyses for all calculated AuL_3 (L = H, F, Cl) compounds show both large Au(5d) and Au(6p) participation in the Au–L bond (Table V). However, hybridization models often fail to predict molecular structures. We therefore studied the importance of d- and p-participation in AuH_3 in more detail. We first excluded Au(5d) participation in the Au–H bond by using a relativistic one-electron pseudopotential for gold with a [Pt]-core definition (the pseudopotential parameters and the exponents for the gold (7s/3p/1d) basis set used are given in ref 44). We optimized the H_aAuH_e angle at the HF level, keeping the Au–H bond lengths constant by use of the RHF values listed in Table III. The result is a H_aAuH_e angle of ~76° (compare with 87° obtained with the more accurate [Xe4f^{14}]-core definition for gold; Table III). Using equal bond lengths (mean value of 1.57 Å) for all Au–H bonds increases the H_aAuH_e angle only slightly (~0.6°). If we do not include Au(6p) functions in our AuH_3 geometry optimization, a slightly increased H_aAuH_e angle of ~76° is obtained. In all cases, the trigonal planar AuH_3 arrangement

(42) (a) Einstein, F. W. B.; Rao, P. R.; Trotter, P. R.; Bartlett, N. *J. Chem. Soc. A* **1967**, 478. (b) Zemva, B.; Lutar, K.; Jeshi, A.; Casteel, W. J.; Wilkinson, A. P.; Cox, D. E.; VonDreele, R. B.; Borrmann, H.; Bartlett, N. *J. Am. Chem. Soc.* **1991**, *113*, 4192.
(43) Syrkin, Y. K.; Dyatkina, M. E. *Structure of Molecules and the Chemical Bond*; Butterworths Scientific Publ.: London, 1950.
(44) Schwerdtfeger, P. Thesis, Stuttgart, 1986.

did not represent a local minimum or a transition state; i.e., the energy gradient of the H_aAuH_e bending mode is nonzero at 120°. We therefore conclude that the T-shaped structure of AuH_3 (and presumably of AuF_3 and $AuCl_3$) is not simply due to Au(5d) and Au(6p) admixtures in the σ-Au–L bond. Hence, structures of AuL_3 compounds cannot be predicted with use of hybridization models. Electrostatic arguments would predict a trigonal planar arrangement for all AuL_3 compounds due to the electrostatic repulsion of the equally charged ligands. One can, however, rationalize the T-shaped structures by examining the frontier orbitals of AuH_3. As seen from Figure 4, AuH_3 in the $D_{3h}(^1E')$ structure has two electrons in a doubly degenerate e′ orbital, which splits by H_aAuH_e bending into a doubly occupied b_2 (HOMO) and an empty a_1 (LUMO) orbital in the distorted $C_{2v}(^1A_1)$ symmetry. This is a first-order Jahn–Teller distortion, which causes a decrease in total electronic energy and a change in $\alpha(H_aAuH_e)$ of ~34° at the RMP2 level. Hence, AuH_3 is similar in electronic structure to $Au(CH_3)_3$, which has been predicted to undergo a Jahn–Teller distortion.[21] It is easy to verify that a first-order Jahn–Teller distortion is also the reason for the T-shaped structures of AuF_3 and $AuCl_3$.

The dimerization of AuL_3 can easily be visualized as the bridging of the equatorial ligands in the T-shaped AuL_3 units:

Differences in the gross atomic charges in $q(Cl_a)$ and $q(Cl_e)$ are small and almost zero in $AuCl_3$ at the relativistic level, –0.06 (Cl_a) and +0.07 (Cl_e). The gross atomic charge at the Au atom in Au_2Cl_6 is also relatively small (q(Au) = 0.14; Table V). We therefore assume that the Au–Cl_e bond between different $AuCl_3$ units is highly covalent and is not primarily an electrostatic interaction. Dipole–dipole interactions ($\mu(AuF_3)$ = 3.36 D and $\mu(AuCl_3)$ = 0.88 D at the RHF level; Table III) between AuL_3 units would result in a polymeric chain structure. AuF_3 shows very large charge separations between the gold center and the fluorine ligands; i.e., at the relativistic level we calculate for the gross fluorine charges –0.34 (F_a) and –0.46 (F_e). The largest negative charge is calculated for the equatorial fluorine ligand. Electrostatic interactions therefore suggest a polymeric structure with an Au–F_e bridging between different AuF_3 units, resulting in a cis corner-linked polymer of $[AuF_4]$ squares (the fluorine ligands have been labeled to underline the original equatorial (e) and axial (a) positions of the AuF_3 units; compare to Figure 1 of ref 42):

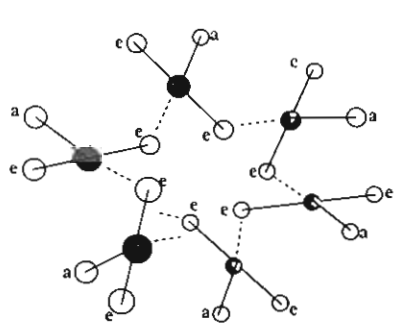

This arrangement can lead to a cyclic geometry between AuF_3 units and may rationalize the helical structure in $(AuF_3)_n$ (bridging via Au–F_a units would result in trans corner-linked squares of $[AuF_4]$ units in which a helical structure would be difficult to adopt). The large positive charge at the Au atom of Au_2F_6 (q(Au) = 1.47; Table V) and the large negative charge at the fluorine atoms allow cross-linked electrostatic interactions between F and Au atoms in different AuF_3 chains. RHF results on the AuF_3 dimerization energy suggest that the interaction between different

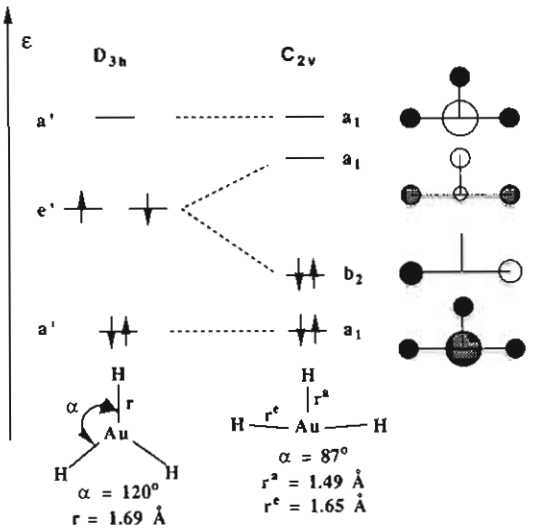

Figure 4. Schematic diagram of the first-order Jahn–Teller distortion in the four frontier orbitals of AuH_3. The Au(6s)–H(1s) linear combinations for the different irreducible representations in the C_{2v} point group are shown on the right-hand side.

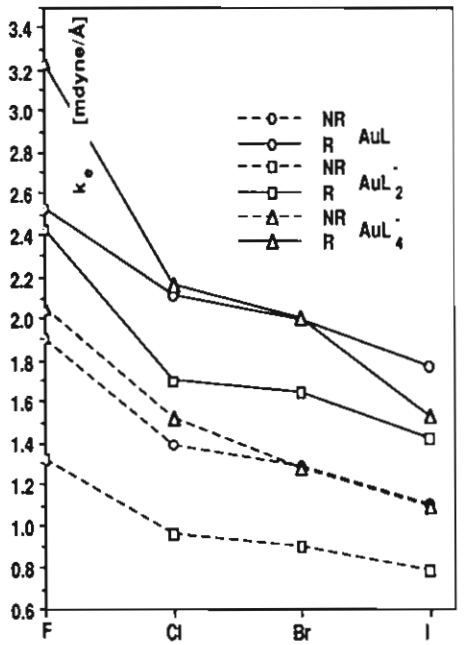

Figure 5. MP2 symmetric Au–L bond stretching force constants for AuL, AuL_2^-, and AuL_4^- in mdyn/Å (L = F, Cl, Br, I).

AuF_3 units is quite large (Table VI). In the nonrelativistic case $AuCl_3$ also shows larger charge separations, i.e. –0.10 (Cl_a) and –0.41 (Cl_e), and it is doubtful if the dimeric structure would be more stable than possible polymeric arrangements at the nonrelativistic level. Hence, electrostatic interactions between Cl and Au atoms in different $AuCl_3$ units are expected to be small, which may explain why this compound does not polymerize.

B. Force Constants. The AuL_4^- force constants are plotted in Figure 5. The optimization of the Au–L bond distances has been carried out simultaneously for all four Au–L bonds.[45] Relativistic effects in the symmetric Au–L stretching force constants are rather large ($\Delta_R k_e$ = –0.4 to –1.2 mdyn/Å at the MP2 level; Table IV) and of the same magnitude as those in the previously discussed Au(I) compounds. The change in the internuclear repulsion term per Au–L bond caused by the relativistic

(45) The Au(III) halide complexes are rather unstable at the HF level (Table I). We therefore varied two of the four Au–L bond distances in the trans position of AuL_4^- keeping the other two Au–I bonds fixed, which resulted also in a minimum.

Table VIII. Experimental[28-31] and Calculated Frequencies (Lower Column) from a Simple Harmonic Valence Force Field for AuL_4^- Compounds (L = F, Cl, Br, I) in D_{4h} Symmetry (in cm^{-1}) Using Program VIB[32] [a]

L	method	$\nu_1(A_{1g})$	$\nu_2(B_{1g})$	$\nu_4(B_{2g})$	$\nu_6(E_u)$	$\nu_7(E_u)$	f_r	$f_r(A_{1g})$	f_{rr}	$f_{rr'}$	f_α	$f_{\alpha\alpha'}$
F	exptl	588	233	561								
	calc	588	233	561	592	210	3.49	3.88 (3.24)	0.09	0.21	0.18	(-0.03)[b]
Cl	exptl	347	171	324	350	179						
	calc	345	171	324	350	160	2.10	2.48 (2.17)	0.07	0.24	0.18	-0.03
	exptl	349	172	325	361	166						
	calc	349	172	325	361	160	2.18	2.54 (2.17)	0.08	0.20	0.18	-0.03
Br	exptl	212	102	196	252	110						
	calc	212	102	196	252	110	1.78	2.12 (2.00)	0.08	0.18	0.16	-0.02
	exptl	214	106	196	252	106						
	calc	214	106	196	252	106	1.80	2.17 (2.00)	0.09	0.19	0.15	-0.02
I	exptl	148	75	110	192	113						
	calc	150	75	110	192	110	1.19	1.61 (1.53)	0.20	0.11	0.24	-0.02

[a] Calculated Au-L stretching force constants f_r and LAuL bending force constants f_α and corresponding nondiagonal elements f_{rr}, $f_{rr'}$ and $f_{\alpha\alpha'}$ in mdyn/Å. $f_r(A_{1g})$ denotes the symmetric stretching mode ($f_r(A_{1g}) = f_r + 2f_{rr} + f_{rr'}$). Symmetric MP2 Au-L stretching force constants are set in parentheses (from Table I). The notation is according to Nakamoto.[33] [b] Assumed.

bond contraction is smaller than that in the Au(I) compounds (see eq 6 in ref 15), and therefore, one may expect smaller changes in $\Delta_R k_e$ for Au(III) than for Au(I) compounds. This leads to the conclusion that electronic effects play a major role in the increase of k_e; i.e., relativistic effects may increase the covalency in the Au-L bond. This is plausible since the ionic contribution to gold-halogen bonds is diminished through the relativistic increase in the gold electronegativity.[16] The origin of relativistic effects in force constants is theoretically not fully understood at the moment. A detailed analysis of the different electronic contributions to $\Delta_R k_e$ for a series of compounds would be very useful to understand this behavior in more detail. Experimental studies on the vibrational spectra of CuF_4^- and AgF_4^- are not available; the metal-ligand stretching force constants should show the expected trend $k_e(AuF_4^-) > k_e(CuF_4^-) > k_e(AgF_4^-)$. However, vibrational data have been reported for several Au(III) complexes; some of them are collected in Table VIII. From a normal coordinate analysis the symmetric stretching force constants $f_r(A_{1g})$ are found to be in satisfying agreement with our calculated MP2 values. The off-diagonal force constants for the stretching modes are quite large and cannot be neglected. The deviation of the MP2 $k_e(AuL_4^-)$ from experiment is largest in the halide series for L = F. As pointed out previously,[15] accurate force constants for Au-F bonds are rather difficult to calculate and more sophisticated methods for taking electron correlation into account are necessary. This, however, was not feasible because even a single point MP2 calculation for AuF_4^- was extremely CPU time consuming. The stretching force constant for AuI_4^- is rather small compared to the other halides. However, the calculated value is in very good agreement with the adjusted force constant derived from experiment. AuI_4^- has also the lowest bond stability of all Au(III) halide complexes (it is well-known that gold(III) iodide complexes are rather unstable and decompose easily into AuI_2^- and I_2;[46] see the next section). The decreasing trend in Au-L stretching force constants from AuF_4^- to AuI_4^- can be seen at both levels (NR and R). The explanation may lie in a decreasing covalency in the Au-L bond with increasing nuclear charge of the halogen ligand, as is the case for the AuL_4^- series.[2]

$CsAuF_6$ has been analyzed by IR vibrational spectroscopy by Leavy and Bartlett.[28] The IR a_{1g} symmetric Au-F stretching frequency in AuF_4^- is almost identical to that of AuF_6^- ($CsAuF_6$, 595 cm^{-1}; $CsAuF_4$, 588 cm^{-1}). Leavy and Bartlett concluded that the activation of the nonbonding d_{z^2} orbital in $CsAuF_4$ by addition of two more fluorine ligands does not change the Au-F bond strength.[3] This is supported by our results; i.e., the HF or MP2 force constants of AuF_4^- and AuF_6^- are not substantially different (note that off-diagonal force constants have been neglected).

We should note that the relativistic change in the Au-L stretching force constants in AuL_3 and Au_2L_6 compounds are also quite large and cannot be neglected; e.g., at the HF level we calculate for $k_e(Au-Cl_c)$ of Au_2Cl_6 1.97 mdyn/Å (NR) and 2.54 mdyn/Å (R), respectively. There are, however, no vibrational data available for this compound to compare with.

C. Bond Stabilities. The dissociation energies of all calculated molecules are collected in Tables I-IV, VI, IX, and X. These values are not corrected for zero point vibration contributions (ZPVC), which can be quite significant. For example, we calculate 18 kJ/mol ZPVC for the dissociation $AuF_4^- \rightarrow Au + 3F + F^-$ using the seven calculated frequencies listed in Table VIII (the ZPVC for the other halides are smaller due to increasing mass of the halide ligand as well as decreasing Au-L stretching force constants in the series from F to I; Table VIII). The halides follow the stability sequence $AuF_4^- > AuCl_4^- > AuBr_4^- > AuI_4^-$ in agreement with experimental findings[2] and in agreement with the overall decrease in the Au-L stretching force constant along this series. Note that AuF_4^- shows a large relativistic stabilization in the Au-F bond (Table IV) in contrast to the molecule AuF;[16] the latter molecule has not been synthesized so far. The relativistic increase in the dissociation energy decreases from AuF_4^- to AuI_4^-. This agrees with the fact that AuI_4^- is very unstable and decomposes easily into AuI_2^- and I_2.[46] Figure 6 shows the changes in internal energy ΔU_0 for the decomposition

$$AuL_4^- \rightarrow AuL_2^- + L_2 \qquad (1)$$

at various levels of electron correlation. Electron correlation as well as relativistic effects play a very important role in the decomposition reaction 1; e.g., at the RMP2 level electron correlation increases ΔU_0 by about 120 kJ/mol for AuI_4^-, while relativistic effects also increase ΔU_0 by about 105 kJ/mol in this compound. MP3 and MP4 results are quite similar, indicating that the MP series is converging relatively fast for this reaction (compare to Raghavachari and Trucks[47] for results on other transition elements). The most important result from Figure 6 is that the oxidation state +3 in gold is clearly supported by relativistic effects. At the RMP4 level all ΔU_0 values are positive. This is not the case for the NRMP4 results. This suggests that the high stability of gold compounds in the oxidation state +3 relative to copper or silver is a relativistic effect, as stated before by using simple HF calculations (in fact, HF describes the trend correctly along the series AuF_4^-, $AuCl_4^-$, $AuBr_4^-$, and AuI_4^-).[18] ΔU_0 for reaction 1 follows the sequence $AuF_4^- > AuCl_4^- > AuBr_4^- > AuI_4^-$ (Table IX), suggesting that the preference for oxidation state +3 should be most evident in the gold(III) fluorides and least in the gold(III) iodides, as observed experimentally.[2] It is interesting to note that the addition of an F^- anion to AuF_3 releases a large amount of bonding energy, ~500 kJ/mol at the RHF level. If we compare to the smaller value for the AuF_3 dimerization energy, it becomes evident why reactions like $AuF_3 + RF \rightarrow R^+[AuF_4^-]$ are exothermic.[2]

(46) Ryan, J. L. *Inorg. Chem.* **1969**, *8*, 2058.

(47) Raghavachari, K.; Trucks, G. W. *J. Chem. Phys.* **1989**, *91*, 1062.

Table IX. MP Reaction Energies for the Dissociations $AuL_4^- \rightarrow AuL_2^- + 2L$ (Spin–Orbit-Corrected D_e Values in Parentheses) and $AuL_4^- \rightarrow AuL_2^- + L_2$ (ΔU_0) in kJ mol^{-1} (L = F, Cl, Br, I)[a]

		D_e				ΔU_0			
L	method	HF	MP2	MP3	MP4	HF	MP2	MP3	MP4
F	NR	−81.3	371.3	238.2	240.3	70.6	219.4	148.0	147.8
	R	116.6	488.9	393.8	396.0	268.5	337.0	303.6	303.5
		(113.7)	(485.7)	(390.6)	(392.8)				
	Δ_R	−197.9	−117.6	−155.6	−155.7	−197.9	−117.6	−155.6	−155.7
		(−195.0)	(−114.4)	(−152.4)	(−152.5)				
Cl	NR	−100.1	225.2	162.2	141.7	−158.8	24.2	−20.5	−19.6
	R	80.3	340.8	284.4	274.3	21.6	139.8	101.7	113.0
		(73.3)	(333.8)	(277.4)	(267.3)				
	Δ_R	−180.4	−115.6	−122.2	−132.6	−180.4	−115.6	−122.2	−132.6
		(−173.4)	(−108.6)	(−115.2)	(−125.6)				
Br	NR	−110.6	190.7	134.3	119.0	−197.7	5.3	−38.8	−47.3
	R	−13.3	302.9	244.1	239.2	−41.0	121.1	76.8	77.9
		(−42.1)	(273.5)	(214.7)	(209.8)				
	Δ_R	−97.3	−112.2	−109.8	−120.2	−156.7	−115.8	−115.6	−125.2
		(−152.7)	(−82.2)	(−80.4)	(−90.8)				
I	NR	−151.5	148.0	90.3	78.2	−216.8	−20.7	−65.5	−72.4
	R	−38.9	236.1	165.0	171.3	−87.7	81.1	21.7	32.8
		(−99.6)	(175.5)	(−104.4)	(110.7)				
	Δ_R	−112.6	−88.1	−74.7	−93.1	−129.1	−101.8	−87.2	−105.2
		(−51.9)	(−27.5)	(−14.1)	(−32.5)				

[a] The MP3 and MP4 energies have been calculated at the MP2 bond distances of AuL_4^- and AuL_2^-, respectively (see Tables I and II). The L_2 dissociation energies have been taken from Table X.

Table X. MP2-4 Molecular Properties for the Halogen Dimers L_2 (L = F, Cl, Br, I)[a]

	ligand	HF	MP2	MP3	MP4	exptl
r_e	F	1.332	1.416	1.404	1.408	1.412
	Cl	2.015	2.040	2.051	2.050	1.988
	Br	2.286	2.313	2.328	2.327	2.281
	I	2.699	2.723	2.742	2.741	2.666
D_e	F	−151.9	133.4	90.2	92.5	160.1
	Cl	58.7	201.0	182.7	176.1	242.6
	Br	57.2	181.8	167.3	161.3	192.1
		(66.4)	(185.4)	(173.1)	(166.3)	
	I	48.8	155.0	143.3	138.5	150.1
		(65.3)	(168.7)	(155.8)	(150.6)	
k_e	F	8.72	5.11	5.36	5.27	4.70
	Cl	3.78	3.25	3.07	3.09	3.23
	Br	2.90	2.50	2.32	2.33	2.46
	I	1.97	1.74	1.60	1.60	1.72

[a] Bond distance r_e in Å, dissociation energy D_e in kJ mol^{-1}, and force constants k_e in mdyn Å^{-1}. Experimental values are from ref 26. For Br_2 and I_2, relativistic and nonrelativistic pseudopotentials have been used (not spin–orbit corrected[b]) and the nonrelativistic D_e values are set in parentheses. [b] To compare with experimentally obtained dissociation energies, the atomic spin–orbit contributions should be subtracted, which are ΔE^{SO} = 3 kJ/mol for F_2, ΔE^{SO} = 7 kJ/mol for Cl_2 (from ref 3), ΔE^{SO} = 35 kJ/mol for Br_2, and ΔE^{SO} = 61 kJ/mol for I_2 (from ref 27).

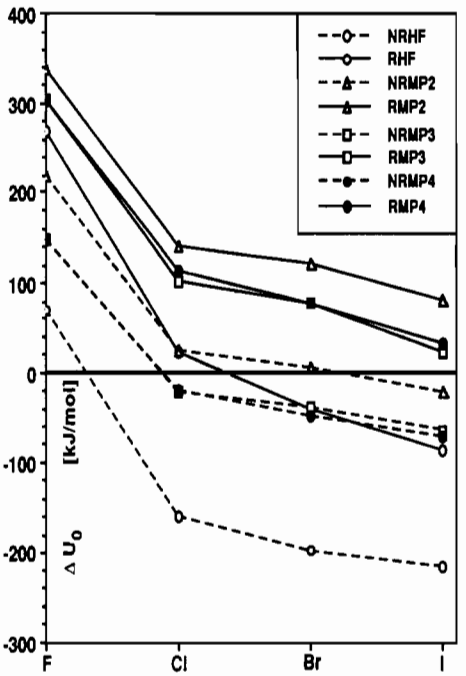

Figure 6. Decomposition energy ΔU_0 (in kJ/mol) of AuL_4^- compounds: $AuL_4^- \rightarrow AuL_2^- + L_2$ at various levels of approximation.

We point out that the dissociation energies for the diatomic halides considerably underestimate the experimental values. This, however, does not mean that the reaction energies of (1) will be influenced greatly by this effect; e.g., see the discussion in ref 48. To achieve higher accuracies, large basis sets, spin–orbit coupling at the molecular level,[27] and high-level configuration interaction are necessary, as done previously for a series of bromine compounds by McGrath and Radom using G1 theory.[49] Such a procedure is not yet feasible for AuL_4^- compounds.

The preference of oxidation state +3 caused by relativistic effects can also be seen in the dissociation energies of the compounds AuL_3 and Au_2L_6 (L = H, F, Cl; Tables III and VI). For example, the reaction energy in the disproportionation

$$6AuCl \rightarrow Au_2Cl_6 + 2Au_2 \qquad (2)$$

changes by about 110 kJ/(mol of AuCl) due to relativistic effects in favor of the production of Au_2Cl_6. This, however, is partly due to the relativistically increased dissociation energy of Au_2 (see ref 16). We assume that correlation energy will result in an exothermic reaction 2, even if we take the production of solid gold into account (the cohesive energy of gold is also relativistically increased[16,50]). This is observed experimentally; i.e., AuCl slowly disproportionates to gold and Au_2Cl_6.[2] The fluorination of gold also yields directly $(AuF_3)_n$ and not the species AuF, in accordance with the relatively low relativistic ΔU_0 value for the AuF disproportionation to $(AuF_3)_n$ (Table VI).

With the MP2 dissociation energies listed in Tables I and II we can discuss the stability of Au(I) complexes due to the disproportionation reaction 3. We define the change of internal energy of the first reaction as ΔU_0 and $\Delta U_0'$ when the gold dimerization energy is included (last reaction in (3)). We obtain the following RMP2 results for ΔU_0 in kJ/mol ($\Delta U_0'$ values are set

(48) Schwerdtfeger, P.; Heath, G. A.; Dolg, M.; Bennett, M. A. *J. Am. Chem. Soc.*, in press.
(49) McGrath, M.; Radom, L. *J. Chem. Phys.* **1990**, *94*, 511.
(50) Takeuchi, N.; Chan, C. T.; Ho, K. M. *Phys. Rev. B* **1989**, *40*, 1565.

$$3AuX_2^- \rightarrow AuX_4^- + 2X^- + 2Au \rightarrow AuX_4^- + 2X^- + Au_2 \quad (3)$$

in parentheses): X = F, 822 (639); X = Cl, 770 (587); X = Br, 740 (557); X = I, 754 (571). These values all show large positive $\Delta U_0'$ values; hence, the Au(I) complexes should be stable due to disproportionation. However, these values represent gas-phase data and high solvation energies for the X^- anions may shift reaction 3 to the right-hand side. We therefore conclude that AuF_2^- may be prepared in nonpolar solvents at low temperatures (to avoid entropy effects), e.g. using organic cations instead of Na^+ or K^+ and organic solvents.[51]

To compare the stabilities of the different halides in their different oxidation states, we consider the halide-exchange reaction

$$AuF_4^- + 2AuX_2^- \rightarrow AuX_4^- + 2AuF_2^- \quad (4)$$

which should be less dependent on solvent, solid-state, and electron correlation effects. The data listed in Tables I and II yield the following results (in kJ/mol at the RMP2 level): X = Cl, 48; X = Br, 52; X = I, 93. This is what we expect from the chemistry of the gold halide complexes; e.g., both AuF_4^- and AuI_2^- are favored species and the reaction energy of (4) is positive.

There have been unsuccessful attempts by Wiberg and Neumaier in 1965 to prepare AuH_3.[52] The T-shaped structure of AuH_3 (Table III) suggests that this compound would dimerize or form a polymeric structure, $(AuH_3)_n$, like $(AuF_3)_n$ or Au_2Cl_6. To discuss the stability of AuH_3, we therefore examine the changes in internal energy ΔU_0^1, ΔU_0^2, and ΔU_0^3 for reactions 5–7

$$Au_2H_6 \rightarrow 2AuH_3 \quad (5)$$

$$2AuH_3 \rightarrow 2AuH + 2H_2 \quad (6)$$

$$2AuH \rightarrow Au_2 + H_2 \quad (7)$$

(neglecting zero-point vibrational contributions). The last reaction can be calculated from experimental values,[26] ΔU_0^3(exptl) = –33 kJ/mol (zero-point vibrational energy correction ZVEC is only –0.1 kJ/mol and can be neglected[26]). This compares reasonably well with the calculated MP2 values (ZVEC neglected), ΔU_0^3(RMP2) = –71 kJ/mol and ΔU_0^3(NRMP2) = –182 kJ/mol[53] (MP2 values in kJ/mol: for AuH, D_e = 270 (R), D_e = 176 (NR), experimental value = 324;[26] for Au_2,[53] D_e = 183 (R), D_e = 106 (NR), experimental value = 223;[26] for H_2, D_e = 428, experimental value = 458[26]). Reaction 6 has also been investigated at the MP2 level; i.e., from Table III we obtain ΔU_0^2(RMP2) = –156 kJ/mol and ΔU_0^2(NRMP2) = –438 kJ/mol. The HF values for these reactions are much lower than the MP2 results, ΔU_0^2(RHF) = –357 kJ/mol, ΔU_0^2(NRHF) = –705 kJ/mol, ΔU_0^3(RHF) = –110 kJ/mol, and ΔU_0^3(NRHF) = –189 kJ/mol. This shows the importance of correlation effects for d-group elements in such reactions, in contrast to similar main-group chemistry investigated recently.[48] Reaction 3 is quite consuming in computer time, so we can give only the HF value, ΔU_0^1(RHF) = 207 kJ/mol. If we consider the overall stability of Au_2H_6, i.e. if we chose $\Delta U_0 = \Delta U_0^1$(HF) + ΔU_0^2(MP2) + ΔU_0^3(MP2), we obtain –20 kJ/mol for the relativistic case. This is still exothermic but could change if a higher level of correlation were used. Thus, it is not clear from thermodynamic arguments if a gold(III) hydride can be isolated.[54] However, AuH_4^-, isoelectronic with the known complex PtH_4^{2-},[55] seems to be quite stable (Table I) and may be prepared.

AuF_6^- is prepared by direct fluorination of $CsAuF_4$.[28] At the RMP2 level we obtain the reaction energy for this fluorination ($AuF_4^- + F_2 \rightarrow AuF_6^-$) of about –132 kJ/mol (–70 kJ/mol at the NRMP2 level), which is exothermic, thus explaining why AuF_6^- is more stable than AuF_4^-. As in the case for the AuF_4^- decomposition, electron correlation plays a very important role in this reaction and HF would result in an endothermic reaction energy of 109 kJ/mol at the relativistic level (280 kJ/mol at the NRHF level).

D. Orbital Energies and Populations. The sequence of HF orbital energies (Figure 7) in Au(III) complexes is significantly different from those previously obtained by ligand field theory or semiempirical methods.[56–59] Except for the fluoride AuF_4^- the ordering for the Au(5d) orbitals is $b_{1g} > e_g \sim a_{1g} > b_{2g}$. However, HF orbital energies are most useful for the interpretation of photoelectron spectra, since HF orbital energies are related to ionization potentials via Koopmans theorem (note, however, that spin–orbit coupling is important in the lower 5d part of Figure 7). For example, some of the gold(IV) halides, AuL_4, are predicted to undergo Jahn–Teller distortions from D_{4h} to D_{2h} (rhombus), since ionization out of the HOMO in the gold(III) halide complexes AuL_4^- may result in a hole in an e_g or e_u orbital (see supplementary material). Similar effects are expected in the gold(VI) fluoride AuF_6.

There is only little work on photoelectron spectroscopy of Au(III) compounds. Mason and Gray assigned $A_{1g} \rightarrow X$ transitions in AuL_4^- complexes for various excited states X.[56] There have been some arguments in the past whether the electronic spectra of AuL_4^- complexes contain Au(d)-to-Au(d) transitions in the lower energy bands.[46,56] We calculated strong Au(5d) admixture in the orbitals lying in the upper part of the energies shown in Figure 7. This supports at least part of the d–d band assignments.[46,56] However, there is large ligand p admixture in the first few HOMOs, which leads to an overall increase in orbital energies from F to I. This increase can be observed experimentally in the decrease in wavenumbers of the charge-transfer bands in AuL_4^- from L = F to L = I.[2,56]

The relativistic 6s stabilization as well as the relativistic 5d destabilization in gold can be nicely seen in Figure 7. Due to relativistic effects, the a_{1g} orbital, which contains mostly Au(6s), decreases energetically, while the lower Au(5d) part increases. The other orbitals, which contain less 6s and 5d, are almost unchanged when changing from NR to R. Therefore, relativistic effects lower the 5d–6s gap in AuL_4^-, as is also the case for AuL_2^- discussed recently.[15] This leads to an increase in the Au(5d) participation in the Au–L bond, which shows up in the population analysis (Table V). Also Au(6p) admixtures in the Au–L bond of Au(III) compounds are remarkably high, as shown in Table V. A comparison with previous results[15,16] gives the sequence in Au(5d) and Au(6p) contributions in the Au–L bond, $AuL_4^- > AuL_2^- > AuL$. The magnitude of Au(5d) and Au(6p) participation in the Au–L bond is strongly dependent on the nature of

(51) Bennett, M. A. Personal communication.
(52) Wibert, E.; Neumaier, H. *Inorg. Nucl. Chem. Lett.* **1965**, *1*, 35.
(53) (a) Schwerdtfeger, P. Unpublished results. (b) Schwerdtfeger, P. *Chem. Phys. Lett.* **1991**, *183*, 457.
(54) For a proper discussion one should consider transition states for the H_2 abstraction of Au_2H_6. We cannot give a nonrelativistic value for ΔU_0^1(HF), because we did not find a minimum for Au_2H_6. A very CPU time-consuming geometry optimization led to a AuH dimer with two loosely bound hydrogen molecules. This also predicts another interesting effect, namely that AuH may dimerize in the gas phase (Cu_2H_2 has been measured in the gas phase: Hauge, R.; Kafafi, Z. H.; Margrave, J. L. In *Physics and Chemistry of Small Clusters*; Jena, P., Rao, B. K., Khanna, S. N., Eds.; Plenum: New York, 1987; p 787.
(55) Bronger, W. *Angew. Chem., Int. Ed. Engl.* **1991**, *30*, 759; *Angew. Chem.* **1991**, *103*, 776.
(56) (a) Mason, W. R.; Gray, H. B. *J. Am. Chem. Soc.* **1968**, *90*, 5721. (b) Mason, W. R.; Gray, H. B. *Inorg. Chem.* **1968**, *7*, 55.
(57) Brown, D. H.; Smith, W. E. *J. Chem. Soc., Dalton Trans.* **1976**, 848.
(58) Basch, H.; Gray, H. B. *Inorg. Chem.* **1967**, *6*, 365.
(59) Zwanziger, H.; Reinhold, J.; Hoyer, E. *Z. Chem.* **1975**, *15*, 69.

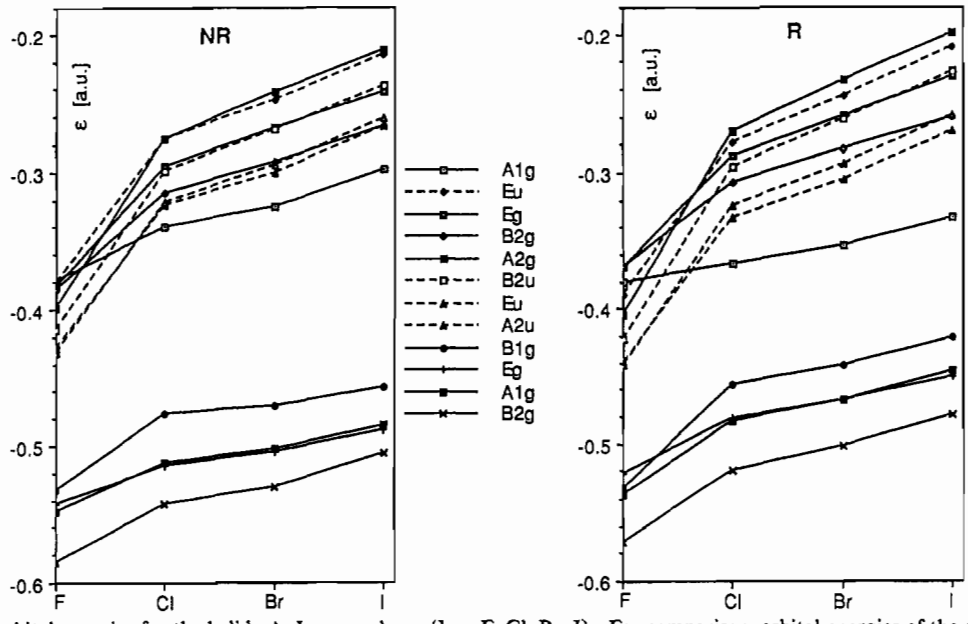

Figure 7. Valence orbital energies for the halide AuL_4^- complexes (L = F, Cl, Br, I). For comparison, orbital energies of the gold atom in the same basis set (in au) are as follows: NR, –0.522 (5d), –0.223 (6s); R, –0.463 (5d), –0.290 (6s).

the ligand, e.g., within the halide series AuL_4^- (L = F, Cl, Br, I) we calculate the magnitude of Au(5d) contributions $AuF_4^- > AuCl_4^- > AuBr_4^- > AuI_4^-$ consistent with the decreasing electronegativity of the ligand L. However, Au(6p) contributions follow the opposite trend compared to Au(5d), as pointed out and discussed before for the gold(I) halide complexes.[15] Relativistic effects significantly increase the magnitude of Au(5d) as well as Au(6p) participation in almost all calculated compounds. The increased relativistic Au(6p) population is difficult to rationalize since relativistic effects increase the gold 6s–6p orbital gap. However, our calculations are qualitatively consistent with earlier SCCC calculations,[20] which also show large Au(6p) populations in Au(III) compounds. This may also be seen as consistent with earlier assumptions of dsp^2 hybridization in square planar Au(III) compounds.[2]

The $^1E'$ state in a D_{3h} molecule is Jahn–Teller active.[60] Figure 4 shows a schematic orbital diagram of a first-order Jahn–Teller distortion in trigonal planar AuH_3. The doubly degenerate e' orbital splits into a b_2 and an a_1 level; the major Au(6s) and H(1s) linear combinations are given in Figure 4. The LCAO drawings show that the lowest occupied a_1 level can be stabilized by Au($5d_{z^2}$) contributions, while the b_2 HOMO can be stabilized by Au($6p_y$) contributions (the molecule is defined in the *zy* plane). A detailed discussion of orbital contributions can be found in the papers of Hoffmann and co-workers[21] on R_3Au compounds (R any organic group), which are very similar to AuH_3. Note, however, that Au(5d) and Au(6p) involvement in the Au–L bond[21] is not necessary to rationalize this Jahn–Teller distortion, as discussed above. The Jahn–Teller effect stabilizes AuH_3 by ~204 kJ/mol at the RMP2 level, which corresponds to the difference in energy between the $^1E'(D_{3h})$ state and the Jahn–Teller distorted $^1A'(C_{2v})$ state. There have been discussions about the diamagnetism of Au_2F_6 despite a d^8 configuration at the square planar gold atom.[2] The Jahn–Teller distortion nicely explains this fact. In fact, if we fix the symmetry of AuH_3 to the trigonal planar form (D_{3h}), the $^3A'$ state is ~37 kJ/mol (r_e = 1.630 Å) below the $^1E'$ state (r = 1.629 Å) at the RMP2 level. Note that the $^1E'$ state is not a transition state; relaxing the bond distances at α = 120° leads to a $C_{2v}(^1A')$ structure (RMP2) with $r(Au–H_a)$ = 3.924 Å and $r(Au–H_e)$ = 1.587 Å, only 36 kJ/mol below the $^1E'(D_{3h})$ state. This suggests that AuH_3 at α = 120° may not be far away from the dissociation limit into the two radicals AuH_2 and H. In fact, Hoffmann and co-workers[21] showed that the Y-shaped structures of R_3Au compounds correspond to transition states of the channel for the R_2 abstraction. We expect a similar hypersurface for AuH_3.

We should point out that there are some gold compounds known with coordination number 3,[34] such as $[Au(PPh_3)_3]^+$.[61] One phosphine ligand, however, "donates" two electrons to the gold atom in contrast to the anionic halide or hydride ligands. Hence, considering the positive charge of the complex, two more electrons are added to the simple orbital picture shown in Figure 4. The e' orbitals are filled resulting in a $^1A'$ state for $[Au(PH_3)_3]^+$, which is not Jahn–Teller active. We expect therefore a P–Au–P angle of 120°. Beside small distortions, this is indeed the case for all $[Au(PR_3)_3]^+$ complexes measured so far.[34]

AuF_3 and $AuCl_3$ also undergo Jahn–Teller distortions. The orbital pictures are more complex than those of AuH_3, but use of ligand s and p orbitals for the linear combination with Au(6s) again gives a Jahn–Teller-active doubly degenerate e' orbital. The tendency of Jahn–Teller distorted AuL_3 units to dimerize to Au_2L_6 (L = F, Cl) is also seen in the frontier orbitals of these fragments. AuL_3 has a very low-lying Au(5d) acceptor LUMO with some $L_a(p)$ admixture and two nearly degenerate $L_e(p)$ donor HOMOs. AuH_3 is very similar, but the acceptor LUMO consists mainly of Au(6s) and the donor HOMO of $H_e(s)$ contributions (Figure 4). This is seen in the population analysis if we compare AuH_3 with Au_2H_6; e.g., the negative charge at the gold atom increases as a consequence of dimerization of AuH_3. The population analyses show no significant Au–Au interactions in Au_2L_6 compounds (L = H, F, Cl). Even for the very short calculated relativistic Au–Au bond distance of 2.77 Å in Au_2H_6 a negative overlap population was obtained. In general, Au–Au interactions have not been observed when the gold atoms have bridging ligands. As in the case of AuF_3, the fluorine atoms in Au_2F_6 have relatively large negative gross charges (R, $q(F_e)$ = –0.47, $q(F_b)$ = –0.53; compare to NR, $q(F_e)$ = –0.46, $q(F_b)$ = –0.64). This is not the case for Au_2Cl_6 at the relativistic level (R, $q(Cl_e)$ = –0.01, $q(Cl_b)$ = –0.12; compare to NR, $q(Cl_e)$ = –0.20, $q(Cl_b)$ = –0.52).

E. Nuclear Quadrupole Coupling. The calculated HF chlorine and gold electric field gradients q (EFG) for several gold halides are listed in Tables XI and XII. As pointed out earlier,[15] we may

(60) Jotham, R. W.; Kettle, S. F. A. *Inorg. Chim. Acta* **1971**, *5*, 183.

(61) Guggenberger, L. Y. *J. Organomet. Chem.* **1974**, *81*, 271.

(62) Nair, K. P. R.; Hoeft, J.; Tiemann, E. *J. Mol. Spectrosc.* **1979**, *78*, 506.

Table XI. Chlorine HF and MSXα Electric Field Gradients (EFG) q (Eq 8) for AuCl, $AuCl_2^-$, and $AuCl_4^-$ in au[a]

molecule	method	q^R	q^{NR}	$q^R(r_e^{NR})$	Δq_1	Δq_2	$\Delta_R q$	exptl	η^R	η^{NR}
AuCl	HF	−2.360	−1.153	−2.345	+1.192	−0.015	+1.207			
	Xα[b]	−3.798	−2.132				+1.666			
$AuCl_2^-$	HF	−1.496	−0.808	−1.479	+0.671	−0.017	+0.688	(−)1.827[c]		
	Xα	−2.374	−1.566	−2.488	+0.922	+0.114	+0.808			
$AuCl_4^-$	HF	−2.980	−2.935	−3.106	+0.161	+0.116	+0.045		0.147	0.131
	Xα	−3.356	−3.165	−3.511	+0.346	+0.155	+0.191		0.102	0.085
Cl_2	HF		−5.826					(−)6.0 (est)		
	Xα		−6.385							

[a] For comparison we added the EFG of chlorine for Cl_2 within the same basis set at the experimental bond distance of 1.988 Å. The asymmetry parameter η is defined as $\eta = |q_z^{-1}(q_x - q_y)|$. X$\alpha$ calculations are carried out at the calculated MP2 bond lengths (Tables I and II). The experimental electric field gradient for Cl_2 is an estimated value given in ref 62. [b] MSXα calculation did not converge for $q^R(r_e^{NR})$. [c] Reference 63.

Table XII. Gold Electric Field Gradients (EFG) q (Eq 8) for AuL_4^- Compounds (L = F, Cl, Br, I), $AuCl_2^-$, and AuCl in au Using the MSXα Method and the MP2 Bond Distances Listed in Table I

molecule	q^R	q^{NR}	$q^R(r_e^{NR})$	Δq_1	Δq_2	$\Delta_R q$	exptl
AuF_4^-	−1.190	+0.988	+0.247	+0.741	−1.437	+2.178	(−)0.15[a]
$AuCl_4^-$	−2.567	−0.608	−1.070	+0.462	−1.497	+1.959	(−)1.26[a]
$AuBr_4^-$	−2.967	−1.155	−1.690	+0.535	−1.277	+1.812	
AuI_4^-	−3.256	−1.695	−2.152	+0.457	−1.104	+1.561	
$AuCl_2^-$	+6.636	+5.431	+3.213	+2.218	+3.423	−1.205	(+)5.79[b]
AuCl[c]	+1.161	+2.325				+1.164	

[a] For $K[AuCl_4]\cdot H_2O$, see ref. 34, p 235. [b] Reference 64. [c] MSXα calculation did not converge for $q^R(r_e^{NR})$.

separate the relativistic change in q, $\Delta_R q$, into two different relativistic contributions

$$\Delta_R q = \{q^{NR}(r_e^{NR}) - q^R(r_e^{NR})\} - \{q^R(r_e^R) - q^R(r_e^{NR})\} = \Delta q_1 - \Delta q_2 \quad (8)$$

namely a relativistic electronic part Δq_1 and a relativistic bond contraction part Δq_2.

For the chlorine EFG the relativistic contribution resulting from the relativistic bond contraction Δq_2 is small in all three cases, AuCl, $AuCl_2^-$, and $AuCl_4^-$, and may be neglected compared to the total magnitude of q. The relativistic electronic contribution Δq_1 decreases along the series $AuCl > AuCl_2^- > AuCl_4^-$. $AuCl_4^-$ has the largest chlorine EFG, but the smallest $\Delta_R q$ value. The relativistic change in the asymmetry parameter η is very small. This agrees with the trend in relativistic changes of bond distances or dissociation energies (but not force constants) discussed before. Obviously, large Au(6p) and Au(5d) participation in the Au–Cl bond (Table V) also quenches relativistic changes in the Cl EFG. The Xα results are in quite good agreement with the HF values; however, the Xα method probably overestimates relativistic changes $\Delta_R q$ in the chlorine EFG.

The gold Xα EFG for the gold(III) halide complexes as well as for $AuCl_2^-$ and AuCl are listed in Table XII. Δq_2 is not small, and therefore, the Au EFG is very sensitive to small changes in the gold–ligand bond length. The total relativistic effects $\Delta_R q$ are very large; i.e., for AuCl the Au EFG changes by ca. 100%, which explains the unusually large measured ^{197}Au NQCC. There is a remarkable difference in the gold EFGs of the chlorides of Au(I) compared with all the Au(III) compounds (Table XII). Such differences have also been observed in Mössbauer spectra of gold complexes.[34] Further is should be noted that in the series AuF_4^- through AuI_4^- the calculated EFG at the gold nucleus is negative leading to positive values for the nuclear quadrupole coupling constant, whereas in Au(I) complexes the opposite is generally true.[65]

We should point out as in the case for the Cl EFG's the relativistic changes $\Delta_R q$ for the Xα gold EFG's are probably overestimated, whilst HF may underestimate such effects. It is well-known that reasonably large basis sets have to be used for obtaining accurate HF field gradients (see the discussion in ref 14). It is therefore difficult to obtain EFG values at the relativistic level for heavy elements like gold. However, Jansen and Hess[66] recently applied relatively large basis sets within a relativistic spin-free no-pair Hamiltonian for calculations on the gold atom, which would be a suitable method for calculating relativistic effects in EFG's for compounds containing heavy elements.

3. Computational and Experimental Details

Computational Details. The pseudopotentials and basis sets used in this work are described in refs 15 and 16. The pseudopotentials for gold, bromine, and iodine have been adjusted by a multielectron-fit procedure,[16,67] which reproduces very accurately the important valence spectrum of the atoms.[16] The basis sets chosen have been rather large to avoid basis set superposition errors.[16] Only for the molecules Au_2F_6 and Au_2Cl_6 we slightly reduced our basis, neglecting d-polarization functions for the F and Cl atoms, because the geometry optimization became rather time-consuming.[41] The geometries are fully optimized using a Fletcher–Powell procedure within the GAUSSIAN86 program system.[24] The computational details are given in ref 16. Møller–Plesset calculations of the second order (MP2) were carried out for the complexes AuL_4^- (L = F, Cl, Br, I) and AuF_6^- to compare with previously published HF and CI results.[18,22] This method has the advantage of being size consistent, which becomes very important for calculating dissociation energies of polyatomic molecules like $AuL_4^- \rightarrow Au + 3L + L^-$. For this reaction we also carried out MP3 and MP4DQ calculations, but only at the optimized MP2 bond distances. This was necessary since a geometry optimization at the full MP4 level would have been too CPU time-consuming. To determine the nuclear quadrupole coupling constant for ^{197}Au, multiple scattering Xα calculations (MSXα) on AuF_4^-, $AuCl_4^-$, $AuBr_4^-$, and AuI_4^- were carried out using the program XASW of Case and Cook.[25] For the gold halide complexes we used the calculated MP2 bond distances given in Table I. For the Xα calculations on Cl_2 we used the experimental bond length of 1.988 Å given in ref 26.

The performance of the MP method for transition metal compounds has been criticized recently by Raghavachari and Trucks.[47] In contrast, the MP2 method shows reasonable results for most molecules containing main-group elements (see for example ref 48). Gold is a borderline case where d-participation becomes more important in the higher oxidation states of gold. However, CI calculations on AuL_4^- compounds including Au(5d) correlation using accurate basis sets are not yet feasible. On the other hand, MP2 results on Au(I) compounds presented in this paper (Table II) compare quite well with earlier published CI results.[15,16] Moreover, the MP2 values for the AuL_4^- decomposition (Figure 6) are not significantly different from the MP4 results and do not changes the overall trend in the reaction energies, suggesting that the MP2 approximation is quite reliable for Au(III) compounds.

Experimental Details. $AuCl_3$ was synthesized by a modification of the procedure reported for the preparation of AuCl(CO).[68] $HAuCl_4\cdot xH_2O$ (1 g) was stirred in neat thionyl chloride for 3 days. After this time the color of the solid had changed from yellow to orange. The thionyl chloride was removed and the solid $AuCl_3$ dried under vacuum at room temperature.

(63) Boyd, P. D. W.; Schwerdtfeger, P. Unpublished results.
(64) Bowmaker, A.; Whiting, R. *Aust. J. Chem.* **1976**, *26*, 29.
(65) Viegers, T. P. A.; Trooster, J. M.; Bouten, P.; Rit, T. P. *J. Chem. Soc.* **1977**, 2074.
(66) Jansen, G.; Hess, B. A. *Chem. Phys. Lett.* **1989**, *160*, 507.
(67) (a) Andrae, D.; Häussermann, U.; Dolg, M.; Stoll, H. *Theoret. Chim. Acta* **1990**, *77*, 123. (b) Wedig, U. Thesis, Stuttgart, 1988. (c) Dolg, M. Thesis, Stuttgart, 1989.
(68) Belli-Dell'Amico, D.; Calderazzo, F. *Inorg. Synth.* **1986**, *24*, 236.

Crystals suitable for single-crystal X-ray diffraction were grown by vacuum sublimation at 100 °C as dark red rods. The moisture-sensitive crystals were mounted in a Lindemann capillary under the atmosphere of dry nitrogen and positioned on a Nonius CAD-4 diffractometer. Unit cell dimensions were derived from least-squares fits to the observed setting angles of 25 reflections. Monochromatic MoKα (λ = 0.710 69 Å) radiation was used. Crystal alignment and decomposition were monitored throughout the data collection by measurement of three standard reflections every 100 measurements. No nonstatistical variation in intensity was observed. The data were corrected for Lorentz and polarization effects and equivalent reflections averaged. Absorption corrections were applied by the empirical azimuthal scan method.[69] Structure solution by Patterson methods and refinement were carried out using the SHELX-86 and SHELX-76 programs.[70] Neutral-atom scattering factors were used.[71] The final electron density map contains peaks at less than 1 Å from the gold atoms of height 2 e/Å^3. No other peaks were observed in the final difference Fourier map.

4. Summary

We summarize the important results of our calculations: (1) Relativistic bond contractions are much smaller in Au(III) compounds than in Au(I) species, probably due to the dilution of Au(6s) density by Au(5d) and Au(6p) participation in the Au–L bond. (2) Relativistic changes in the force constants are large in Au(III) compounds and cannot be neglected. (3) The oxidation state +3 in gold is stabilized by relativistic effects relative to the oxidation state +1, a fact which cannot be explained by relativistic changes in atomic ionization potentials. (4) Monomeric AuL_3 compounds show T-shaped structures which cannot be explained by simple hybridization or electrostatic models. The reason for the $D_{3h} \rightarrow C_{2v}$ symmetry breaking is a first-order Jahn–Teller distortion which splits the doubly degenerate e′ HOMO into an a_1 and a b_1 orbital; the doubly occupied b_1 orbital undergoes a stabilization resulting in a relatively small L_aAuL_e angle of ca. 90°. The T-shaped AuL_3 units can either dimerize (as this is the case for Au_2Cl_6) or polymerize (as is the case for $(AuF_3)_n$). (5) Relativistic effects in the ^{197}Au EFG are very large at the MSXα level. In contrast, changes in the ligand EFG due to relativistic changes at the Au(III) center are relatively small. Relativistic effects in the ^{197}Au EFG should perhaps be studied in detail on diatomic gold compounds by more sophisticated methods, i.e. by all-electron relativistic HF calculations including electron correlation, to support our findings. (6) $(AuH_3)_n$ may be stable, despite the unsuccessful attempts by Wiberg and Neumaier[50] to prepare this species. AuH_4^- is quite stable, and the synthesis of this compound may be feasible. (7) Au(III) compounds show large Au(5d) and Au(6p) participation in the Au–L bond, the relative magnitude of these admixtures being dependent on the nature of the ligand.

Most of the relativistic effects have been discussed at the HF level. Correlation effects have only been included at the MP level, since configuration interaction (CI) or perturbation procedures higher than second order would have been extremely time-consuming given the present standard of computer technology.[41] However, most of the effects and trends discussed in this paper are very significant even at the HF level, so we expect qualitatively no change in trends by introducing CI. This has been shown, for example, for several diatomic gold compounds.[16]

Acknowledgment. We acknowledge IBM New Zealand Ltd. in Auckland and the ANU Supercomputer Facility in Canberra for grants of computer time. Thanks are due to Michael Dolg for providing part of the basis sets and pseudopotentials and to Pekka Pyykkö, Martin A. Bennett, Graham A. Heath, and Lucien Dubicki for helpful discussions. P.S. is very indebted to the Alexander von Humboldt-Stiftung for financial support in the first two years of this project (1988–1989). We thank the Auckland University Research Grants Committee and the Lottery Science Board for financial support.

Supplementary Material Available: Tables SII–SIV, listing crystal data and details of the structure determination of $AuCl_3$, atom positions, anisotropic thermal parameters, and standard deviations for $AuCl_3$, and valence orbital energies and major atomic orbital contributions for the Au(III) complexes and AuF_6^- (5 pages); Table SI, listing observed and calculated structure factors for $AuCl_3$ (1 page). Ordering information is given on any current masthead page.

(69) North, A. C.; Philips, D. C.; Mathews, F. S. *Acta Crystallogr., Sect. A* **1968**, *24*, 351.
(70) Sheldrick, G. M. SHELXS-86 Crystal Structure Solution Program. Universität Göttingen, West Germany, 1978. Sheldrick, G. M. SHELX-76 Program for Crystal Structure Determination. Cambridge University, England, 1976.
(71) (a) Cromer, D. T.; Mann, J. B. *Acta Crystallogr., Sect. A* **1968**, *24*, 321. (b) Cromer, D. T.; Liberman, D. *J. Chem. Phys.* **1970**, *53*, 1891.